

MODELLING OF THE DEACTIVATION OF POLYMER-SUPPORTED PALLADIUM CATALYSTS IN THE HYDROGENATION OF 4-NITROTOLUENE

Milan KRALIK^{a1}, Roman FISERA^{a2}, Marco ZECCA^b, Angelo A. D'ARCHIVIO^{c1}, Luciano GALANTINI^{c2}, Karel JERABEK^d and Benedetto CORAIN^{c3}

^a Department of Organic Technology, Slovak University of Technology, Radlinskeho 9, 812 37 Bratislava, Slovak Republic; e-mail: ¹ kralik@cvt.stuba.sk ² kralik@checdek.chtf.stuba.sk

^b Dipartimento di Chimica Inorganica, Metallorganica e Analitica, via Marzolo 1, 35131 Padova, Italy; e-mail: mzecca@chim02.chin.unipd.it

^c Dipartimento di Chimica, Ingegneria Chimica e Materiali, Università dell'Aquila, Coppito Due – Via Vetoio, 67010 L'Aquila, Italy; e-mail: ¹ darchivio@axscaq.aquila.infn.it,

² galantini@axscaq.aquila.infn.it, ³ corain@chim02.chinunipd.it

^d Institute of Chemical Process Fundamentals, Academy of Sciences of the Czech Republic, 165 02 Prague 6, Czech Republic; e-mail: kjer@icpf.cas.cz

Received March 16, 1998

Accepted May 18, 1998

The kinetics of the hydrogenation of 4-nitrotoluene over Pd catalysts supported on sulfonated polystyrene and simultaneous deactivation of these catalysts were investigated. Reaction rates of both the hydrogenation and the dissolution of Pd crystallites were related to the total Pd surface. The average radius of ideal spherical crystallites, as determined by X-ray powder diffraction analysis, was taken as the starting value of the crystallite size. Stability of the polymer network was checked by Inverse Steric Exclusion Chromatography (ISEC). The ESR and Static Gradient field Spin Echo (SGSE) NMR spectroscopies were used to assess the accessibility and diffusivity before and after deactivation experiments. Langmuir–Hinshelwood type kinetic models were applied to describe the hydrogenation of 4-nitrotoluene. The kinetic law was incorporated into a more comprehensive model involving also diffusion of reactants inside catalytic particles. Simultaneous treatment of a few sets of kinetic data from batch hydrogenation carried out at 0.25–0.75 MPa yielded reliable values of model parameters. The model showed an increasing rate of dissolution of palladium with decreasing concentration of hydrogen and increasing concentration of 4-nitrotoluene. The latter fact supports the hypothesis that the nitro compound is the oxidant responsible for the dissolution of palladium.

Key words: Hydrogenation; 4-Nitrotoluene; Ion-exchange polymers; Polymer-supported palladium catalysts; Catalyst deactivation; Heterogeneous catalysis.

This paper follows a previous report from our laboratories concerning the deactivation of heterogeneous palladium catalysts during the solid–liquid phase hydrogenation of aromatic nitro compounds¹. We reported that the deactivation is due to the dissolution of palladium and that the rate of this process increases with decreasing concentration of hydrogen and increasing temperature.

One of the advantages of polymer-supported catalysts in comparison with inorganic materials is a relatively good accessibility of their inner space. Moreover, transport phenomena are well described especially in the case of microporous, low-crosslinked materials²⁻⁴. In such materials, metal crystallites are accessible from every direction and no correction factors are required to allow for the change of their active surface, as it is the case of metal crystallites deposited onto rigid pore wells of inorganic supports⁵.

Kinetic parameters are usually determined on the basis of data obtained under the so-called kinetic regime^{6,7}. However, quite often the kinetic regime can not be achieved due to the high catalytic activity which makes the resistance to chemical transformation much lower than the resistance to the mass transport. In a previous paper⁴ we described the one-step estimation of both kinetic parameters and diffusion coefficients for the hydrogenation of cyclohexene, upon treatment of several sets of experimental data collected under the diffusion regime at different hydrogen diffusion rates. As quite reliable values of the model parameters were obtained, we have adopted a similar approach to modelling of the catalyst deactivation during the hydrogenation of nitroaromatics.

The stability of the polymer backbone is a very important feature in connection with practical application of polymer-supported metal catalysts. Degradation of the polymer network can arise from a number of sources, including hydrogenolysis, and can eventually lead to its dissolution in the reaction medium. The degradation can increase the accessibility of inner space at first. However, as the process goes on, polymer segments are detached from the backbone and this is a potential source of deactivation; metal crystallites can be fouled and excluded from contact with the reactants. On the other hand, the higher accessibility implies larger separation among the polymer chains, which therefore less effectively protect the metal crystallite from sintering (coagulation in the case of colloids), although this process can be of importance only at relatively high temperatures. Eventually, colloidal metal particles, too fine to be recovered, can be dispersed in solution after complete destruction of the polymer support. The sequence of events described above is in agreement with the activity of polymer-based catalysts going through a maximum during their use: it increases initially as the accessibility of the catalyst improves and then declines as fouling and sintering outweigh the former effect⁸. In order to overcome these drawbacks, many industrial catalysts^{8,9} are based on highly crosslinked polymer materials. These kind of resins are usually macroporous and they are more rigid, but fragile in comparison with low-crosslinked polymers. Moreover, high-crosslinking degrees limit the extent of reagent penetration into the polymer network thus protecting it from degradation.

Inverse Steric Exclusion Chromatography¹⁰ (ISEC) is probably the best method to monitor the changes in the morphology of swollen polymer networks. This method provides the volume distribution of discrete polymer domains as a function of concentration of polymer chains (nm/nm³). The higher the proportion of "dense" domains (concentration of polymer chains equal to 1 nm/nm³ and higher) the stronger the diffu-

sion resistance. Accessibility of swollen polymers may be also evaluated on the basis of rotational mobility as determined from ESR (ref.³) assuming that the translational mobility of molecules is equally affected by the polymer network. We have recently¹¹ tested also Static Gradient field Spin Echo (SGSE) NMR, which proved to be a valuable tool for direct determination of self-diffusion coefficients of swelling media inside swollen polymers.

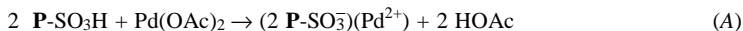
EXPERIMENTAL

Materials

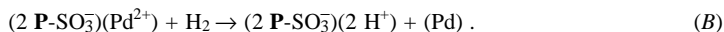
Microporous resin Dowex 50 W × 4 (sulfonated polystyrene with 4 mole % of divinylbenzene as a crosslinker) with particle size 0.16–0.32 mm was used as a support for the Pd catalyst. Palladium acetate (analytical grade) was supplied by Fluka. All other chemicals were supplied by AVOCADO and used as received except cyclohexene which was distilled prior to use.

Catalyst Preparation

The catalysts were prepared from the H⁺ form of Dowex by ion exchange with Pd(OAc)₂ in acetone-water (1 : 1) at room temperature (P denotes the polymer backbone):



followed by reduction with hydrogen in methanol at 50 °C, 1 MPa, 1 h:



The reduced catalyst was eventually washed with methanol and dried in vacuum (5 kPa) at 50 °C. The catalyst was let to swell in a 1 M solution of 4-aminotoluene in methanol for the neutralization of acid sites, prior to use, then washed with methanol and immediately used for experiments.

Characterization of Catalysts

The investigated catalyst was characterized by the following methods:

1. Elemental analysis for palladium¹. The amount of palladium was determined in samples at the start and at the end of catalytic runs.

2. Pycnometric density⁴.

3. Particle size⁴.

4. X-Ray Microprobe Analysis (XRMA) for the assessment of Pd distribution throughout the catalyst particles¹².

5. X-Ray powder diffraction measurements for the estimation of average size of palladium crystallites¹³.

6. ISEC before and after treatment for detection of changes in the morphology of the polymer matrix and determination of swelling volumes, *S* (ref.¹⁰).

7. ESR of a paramagnetic probe confined in the swollen polymeric material for the determination of the rotational correlation time (rotational mobility)³.

8. SGSE NMR of methanol confined in the swollen catalyst for the determination of its self-diffusion coefficient (translational mobility)¹¹.

The experimental procedures used are the same as in the given relevant references.

Catalytic Tests

We used a batch reactor for both the reduction of Pd catalysts and catalytic tests. Hydrogen consumption was monitored by means of a specially designed apparatus¹⁴ connected to the reactor. The runs were carried out at 30 °C and 0.25–0.75 MPa. The reactor was vigorously shaken at a frequency of 12 Hz. A typical reaction mixture consisted of 6 ml of 1 M solution of 4-nitrotoluene in methanol and a weighed amount of catalyst, which was reduced and neutralized by 4-aminotoluene just prior to use. The final conversion of 4-nitrotoluene to 4-aminotoluene in the reaction mixture was determined by gas chromatography. The used catalyst was either taken for palladium analysis or recycled (two recycles at 0.25 and 0.5 MPa and three recycles at 0.75 MPa) after quick washing in methanol and addition of fresh reaction mixture.

The extent of possible side reactions, as suggested by Haber's scheme of the reduction of aromatic nitro compounds¹⁵, was checked for in separate catalytic tests. At approximately 25, 50 and 75% conversion, the cumulative chromatographic area relative to compounds other than 4-nitrotoluene and 4-aminotoluene was less than 1%. This circumstance allowed us to calculate the conversion of 4-nitrotoluene from the hydrogen consumption.

Treatment of the Catalyst in the Reaction Medium

In order to check the stability of the polymer network, the catalysts were treated as follows:

1. Swelling with neat methanol; exposition to hydrogen in the hydrogenation reactor at the same shaking frequency as in the catalytic tests; other conditions are given in Table I.

2. Swelling with 1 M solution of 4-aminotoluene in methanol; then, as above.

3. Swelling with 1 M solution of 4-nitrotoluene in methanol; exposition to nitrogen in the reactor for 6 h, at the same shaking frequency as in the catalytic tests.

Samples of catalyst treated as above were used for the hydrogenation of cyclohexene and 4-nitrotoluene and the reaction half-times¹ were compared with the values obtained over untreated catalysts (Table I). Treated catalysts were also characterized by means of ESR and SGSE NMR techniques. For some of these materials, ISEC measurements were performed.

MATHEMATICAL MODEL OF REACTION KINETICS AND MASS TRANSPORT

Development of the Mathematical Model

The mathematical model was formulated for: (i) isothermal stirred tank reactor, (ii) equilibrium concentration of hydrogen in the liquid bulk and the surface of catalyst particle, (iii) spherical microporous catalyst particles swollen in methanol with homogeneous structure represented by constant diffusivity and concentration of catalytic sites, (iv) equilibrium constants (partition coefficients) of components inside the swollen resin and the liquid bulk equal to 1.

The model also takes into account deactivation of the catalyst according to the hypothesis suggested in ref.¹, *i.e.*, oxidation of Pd(0) to Pd(II) by the nitro compound. The mathematical model is expressed by Eqs (1)–(6).

Material Balances

Component balance in the liquid bulk:

$$\frac{dc_i}{dt} = -\frac{V_P}{V_L} a_p k_{LS} (c_{i,S} - c_{i,L}) \quad (1)$$

Component balance in the particle:

$$\frac{\partial c_i}{\partial t} = \frac{D_i}{\varepsilon_p r^2} \frac{\partial}{\partial r} \left(r^2 \frac{\partial c_i}{\partial r} \right) + \sum_{j=1}^{n_R} \xi_j \nu_{ji} \quad (2)$$

Boundary conditions:

$$\left. \left(\frac{\partial c_i}{\partial r} \right) \right|_{r=0} = 0 ; \quad -D_i \left. \left(\frac{\partial c_i}{\partial r} \right) \right|_{r=r_p} = k_{LS} (c_{i,S} - c_{i,L}) \quad (3)$$

for $i = 1, 2$ (1 for 4-nitrotoluene, 2 for hydrogen).

Initial conditions:

$$c_1(r) = c_{1L,0} \text{ (the particle swollen in the starting reaction mixture);}$$

$$c_2(r) = 0 \text{ (zero concentration of hydrogen at the start); } 0 \leq r \leq r_p \text{ .}$$

Rate equation of hydrogenation of 4-nitrotoluene (the best model):

$$\xi_1 = \frac{s_{Pd}^{a_{Pd}} k_1 c_{H_2}^{0.5} c_{NT}^{a_{NT}}}{(1 + K_{1,H_2}^{0.5} c_{H_2}^{0.5})^2} \quad (4)$$

(the adsorption of 4-nitrotoluene and 4-aminotoluene was neglected)

$$s_{Pd} = n_{Pd,cr} 4\pi r_{Pd,cr}^2 \quad (5)$$

The number of Pd crystallites ($n_{\text{Pd,cr}}$) was calculated from the swelling volume of the catalyst (ISEC), size of Pd crystallites (X-ray powder diffraction) and weight fraction of palladium in the dry catalyst.

Dissolution of palladium:

$$\frac{dr_{\text{Pd,cr}}}{dt} = -k_2 c_{\text{NT}}^{a_2} \exp(-a_{2,\text{H}_2} c_{\text{H}_2}) \quad \text{for } r_{\text{Pd,cr}} > 0 \quad (6)$$

with the initial condition

$$r_{\text{Pd,cr}}(t=0) = r_{\text{Pd,cr},0} \quad (7)$$

Dependence of diffusion coefficients on the swellability:

$$D_i = D_{i,0} \exp\left(-\frac{a_D}{S}\right) \quad (8)$$

Parameter a_D was determined from ESR measurements according to the following expression⁴:

$$\tau_i = \tau_{i,0} \exp\left(\frac{a_D}{S}\right) \quad (9)$$

The reaction order of hydrogen was set to 0.5 in the rate equation (4), which implies dissociative adsorption of hydrogen on the catalyst surface. This assumption is in agreement with literature models^{16,17}. Equation (6), which describes the dissolution of palladium crystallites, is not a “true” kinetic law for the process. According to the reaction scheme we have suggested previously¹, the dissolution of palladium consists of oxidation of palladium metal, formation of palladium(II)–4-aminotoluene complexes and their diffusional transport from the interior of the catalyst particle to the liquid bulk. The occurrence of the last step depends on sterical constraints imposed by the polymer network. Mathematical description of such a complex system requires too many parameters. Moreover, some of these parameters, *e.g.* stability constants of amine complexes and their diffusion coefficients, are unknown. The simplified equation (6) provides only a phenomenological description of the behaviour of palladium metal in polymer catalysts under the experimental conditions. Any direct effect of the concentration of 4-aminotoluene is not involved in Eq. (6). Its presence in large excess with respect to the formation of palladium(II) complexes and fast formation of this complex

are implicitly assumed, so that the formation of palladium–amine complexes is not considered the rate-limiting step.

Parameter Estimation

The following parameters (for their meaning, see Symbols) were estimated: (i) a_{Pd} , (ii) k_1 , (iii) $a_{1,\text{NT}}$, (iv) K_{1,H_2} , (v) k_2 , (vi) $a_{2,\text{NT}}$, (vii) a_{2,H_2} . This was accomplished in a similar way as described previously⁴, *i.e.*, partial differential equations (2)–(4) were converted by the collocation method¹⁸ to a system of ordinary differential equations, which were solved simultaneously together with Eq. (6) by means of the Runge–Kutta–Hanna method¹⁹. Three collocation points were used to assess the accuracy of theoretical conversion curves of 4-nitrotoluene with relative errors less than 0.1% for a wide range of estimated parameters. Experimental conversion curves were fitted by a least-square minimization procedure (Eq. (10)).

$$\text{SSE} = \sum_{j=1}^{n_{\text{rd}}} \sum_{i=1}^{n_{\text{rd},j}} \left(y_{ij}^{\text{meas}} - y_{ij}^{\text{calc}} \right)^2 + w_{\text{st,Pd}} \sum_{j=1}^{n_{\text{rd}}} \left(w_{\text{Pd},j}^{\text{meas}} - w_{\text{Pd},j}^{\text{calc}} \right)^2 \quad (10)$$

The Gauss–Newton–Marquardt method⁷ was applied to the search of the minimum. All of the sets of data obtained at 0.25, 0.5 and 0.75 MPa were treated simultaneously (10 conversion curves, 228 points) and all of the seven (later six) parameters were searched for in the final treatment of data. Searching for the minimum was repeated using also four collocation points in order to confirm the results obtained with three collocation points.

RESULTS AND DISCUSSION

Morphological Changes of Catalysts and Catalytic Activity

The ISEC patterns of the starting polymer support (D4H), the catalyst (D4HPd), the catalysts treated in methanol (tM30, tM50) and 4-aminotoluene (tMA30) are given in Fig. 1. The swelling agent employed for ISEC measurements was 0.1 M aqueous solution of sodium sulfate.

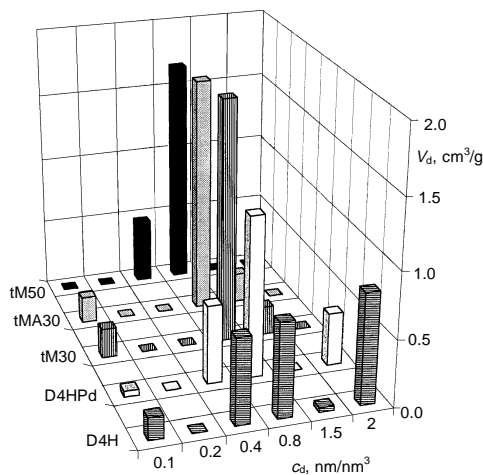
The ISEC data demonstrate an extensive hydrogenolysis of the polymer support during both the reduction of palladium(II) and the catalyst treatment. Moreover, the results indicate that the hydrogenolysis extent is larger when the catalyst is treated under relatively more drastic conditions. The polymer chain density distribution clearly shifts towards lower values going from the support (D4H) to the catalyst treated in methanol at 50 °C. On the other hand, the molecular mobility in methanol, as shown by the measurements of rotational correlation times and self-diffusion coefficients¹¹ (Table I)

is the same in all the investigated materials. At first glance, this finding is rather surprising because the nanomorphology of the support is expected to affect its accessibility. However, the swelling agent employed for ISEC measurements was an aqueous solution of sodium sulfate, whereas the determination of rotational correlation times and self-diffusion coefficients was carried out on materials swollen in neat methanol. Although the swelling power of water and methanol for these polymer materials should be practically the same (see the values of bulk-expanded volumes of Dowex 4 reported in ref.¹), the electrolyte in the mixture for ISEC analysis is expected to reduce substantially the extent of swelling. In fact, it buffers the ionic strength of the solution and suppresses Coulombic repulsions of the fixed ionic charges in the polymer network, which aid in swelling²⁰. Therefore, it is possible that the higher swelling degree of the materials in neat methanol levels off the nanomorphologies of the catalyst to the point that differences in molecular mobility cannot be evaluated under the employed conditions²¹. On the other hand, previous experience showed that ISEC characterization in neat methanol does not yield reliable results^{22,23}.

The values of the reaction half-times of hydrogenation of cyclohexene and 4-nitrotoluene (Table I) show that the untreated catalyst and the materials treated at 30 °C have given practically the same performance. This clearly indicates that at this relatively low temperature and for reaction times not longer than 6 h hydrogenolysis of the polymer support is not a significant cause of deactivation. This also suggests that the mass transport rate is the same for these materials provided that the process does not occur in the kinetic regime. The latter circumstance is also supported by our previous finding that very much smaller particle sizes would be required for the attainment of kinetic regime with 0.5% polymer supported palladium catalysts¹². In contrast, the hydrogenation of cyclohexene was slower over the materials treated at 50 °C. As no deactivation is ex-

FIG. 1

ISEC patterns for the Dowex resin (D4H), the resin with Pd(0) (D4HPd); the catalyst after treatment for 6 h at 30 °C, 0.5 MPa of H₂ in methanol (tM30); the catalyst after treatment for 6 h at 30 °C, 0.5 MPa of H₂, 1 M 4-aminotoluene in methanol (tMA30); the catalyst after treatment for 6 h at 50 °C, 0.5 MPa of H₂ (tM50)



pected to occur during the hydrogenation of the alkene, this finding implies that the catalysts were deactivated during the treatment as a consequence of a fouling of palladium crystallites. Release of colloidal metal particles is ruled out as no palladium loss was observed during these tests.

As far as the hydrogenation of 4-nitrotoluene is concerned, equal values of the reaction half-time were also observed for the untreated catalyst and the materials treated at 30 °C, whereas the materials treated at 50 °C exhibits larger values (the higher the pressure employed for the treatment, the longer the half-time; see entries 5 and 4 in Table I). This finding is in agreement with the hypothesis of partial deactivation during the pre-treatment. However, it is also possible that the deactivation during the hydrogenation of the aromatic substrate is faster for the materials treated at 50 °C than for the other ones.

In conclusion, the results presented in Table I indicate that the catalytic performance is insensitive to morphological changes provided that temperatures lower than 30 °C, pressures below 0.75 MPa and total reaction time shorter than 6 h are applied. Under these conditions, deactivation in the hydrogenation of the nitroaromatics is due only to oxidation of palladium metal by the substrate.

Mathematical Treatment of Catalytic Tests

The content of palladium in the reduced catalyst, determined by elemental analysis was 0.46% (w/w) in the dry material. The XRMA of catalytic particles revealed a homogeneous distribution of Pd crystallites, whereas the average radius of Pd crystallites was

TABLE I
Effect of treatment of catalysts on the mobility of molecules and the catalytic activity^a

Entry	M _t	T _t	P _t	t _t · 10 ⁴	τ _{rc}	D _M · 10 ⁹	τ _{h, cen} ^b	τ _{h, NT} ^c
1(D4H)	water	298	0.1	4.32	193	4.8	—	—
2(D4HPd)	MeOH	323	1.5	0.36	207	4.7	354	1 930
3(tM30)	MeOH	303	0.5	2.16	200	4.9	345	1 870
4(tM50)	MeOH	323	0.5	2.16	200	4.4	392	2 420
5	MeOH	323	0.75	2.16	192	4.3	420	2 60
6(tMA30)	MeOH + 4-AT	303	0.5	2.16	205	4.7	347	1 920
7	MeOH	303	0.75	2.16	202	4.8	352	1 980
8	MeOH	303	0.75	4.32	195	4.7	360	1 920
9 ^d	MeOH + 4-NT	303	0.5	2.16	204	4.6	341	1 990

^a See Symbols for the meaning of the column headers. Materials with names in brackets have ISEC patterns in Fig. 1; ^b 30 °C, 0.5 MPa, [Pd] = 0.5 mol/m³; ^c 30 °C, 0.5 MPa, [Pd] = 1 mol/m³; ^d treatment under nitrogen.

6 nm (X-ray powder diffraction measurements). Other characteristic features of the catalyst are collected in Table II. The diffusion coefficient of 4-nitrotoluene in methanol was calculated as the average of the values obtained by the methods of Hayduk and Minhas, Tyn and Calus, and Wilke–Chang method, respectively, and their modifications as reported in ref.²⁴. The values of estimated parameters are collected in Table III.

The model fitted experimental conversion curves very well, as illustrated by Fig. 2. The average difference between measured and calculated conversion was less than 1.5%.

Figure 3 shows the profiles of average Pd concentration as determined from elemental analyses of the metal and XRMA as compared with those obtained from the mathe-

TABLE II
Values of constant parameters

Parameter	Value	Source
Pycnometric density of the catalyst	1 400 kg/m ²	this paper
Swellability of the catalyst	0.00202 m ³ /kg	ISEC
Porosity of the swollen catalyst, ϵ_p	0.65	this paper
Diffusion parameter, a	0.00352	this paper
Radius of swollen catalyst particles, r_p	0.155 mm	optical microscopy
Radius of Pd crystallites, $r_{Pd,cr}$	6 nm	X-ray powder diffraction
Diffusion coefficient for 4-nitrotoluene, $D_{1,0}$	$1.81 \cdot 10^{-9} \text{ m}^2/\text{s}$	ref. ²⁴
Diffusion coefficient for hydrogen, $D_{2,0}$	$1.7 \cdot 10^{-8} \text{ m}^2/\text{s}$	ref. ²⁵
Hydrogen solubility (MeOH)	0.387 mol/(m ³ MPa)	ref. ²⁶
Liquid–solid mass-transfer coefficient, k_{LS}	–	not taken into account ^a

^a The liquid–solid resistance against the transport of reaction species is negligible in comparison with the resistance against diffusion transport inside the swollen particle.

TABLE III
Estimated parameters (units: kg, m³, kmol, s; errors are evaluated for the 95 % probability level⁷)

Parameter	Value	Parameter	Value
k_1 , $\text{kmol}^{(0.5-a_{1,NT})} \cdot \text{m}^{(-1.5+a_{Pd}+3a_{1,NT})} \cdot \text{s}^{-1}$	$0.12 \cdot 10^{-14} \pm 0.13 \cdot 10^{-17}$	a_{Pd}	$2.8 \pm 37 \cdot 10^{-4}$
$a_{1,NT}$	$0.39 \pm 0.37 \cdot 10^{-5}$	K_{1,H_2} $\text{kmol}^{-1} \cdot \text{m}^3$	$2.56 \pm 0.21 \cdot 10^{-4}$
k_2 $\text{kmol}^{-a_{2,NT}} \cdot \text{m}^{(1+3a_{2,NT})} \cdot \text{s}^{-1}$	$0.94 \cdot 10^{-4} \pm 0.15 \cdot 10^{-8}$	$a_{2,NT}$	1 ^a
a_{2,H_2} $\text{kmol}^{-1} \cdot \text{m}^3$	$0.19 \pm 0.23 \cdot 10^{-5}$		

^a Not estimated, set to unity due to the correlation with other parameters.

mathematical model. The extent of cumulative palladium leaching at 0.75 and 0.5 MPa is comparable, because at the higher pressure, four runs, instead of three, were carried out with the same catalyst batch. The calculated profile shows that dissolution proceeds to a greater extent close to the particle edges than in the core. This is in agreement with the hypothesis that dissolution is faster when the concentration of 4-nitrotoluene is higher. However, the hydrogen concentration at the edge of the particles is higher than in the center and this prevents the dissolution of palladium to proceed much faster than in the center, both directly (according to Eq. (6), H_2 is an inhibitor of this reaction) and indirectly (nitrotoluene is consumed). As a result, the palladium concentration is only slightly lower at the edge than in the center of the particles.

The hydrogenation of 2,4-dinitrotoluene over Pd supported on carbon indicated that deactivation stops when the kinetic regime is achieved¹⁶. The kinetic regime is reached because in the partially deactivated catalyst the chemical reaction is sufficiently slow that the transport of hydrogen to catalytic sites is no longer the limiting process. Under

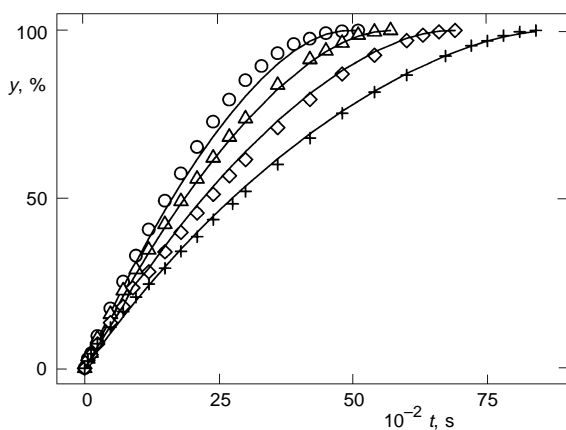


FIG. 2

Measured (symbols) and calculated (solid lines) conversion curves in the batch hydrogenation of 4-nitrotoluene at 30 °C, 0.75 MPa, $[Pd] = 1$; 3 recycles of the catalyst: 0 (○), 1st (Δ), 2nd (◇), 3rd (+)

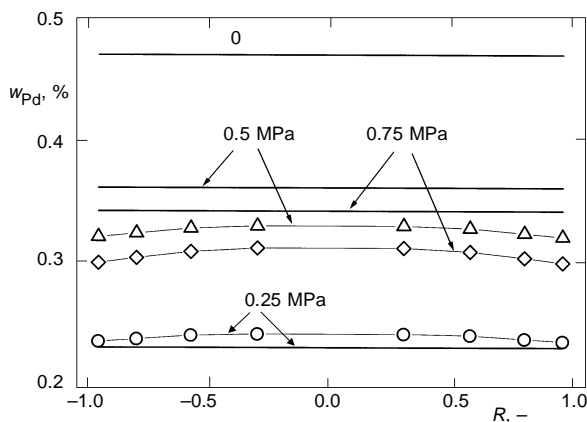


FIG. 3

Calculated distribution profiles (symbols) of palladium weight percentage across catalyst particles after the batch hydrogenation of 4-nitrotoluene carried out at 30 °C and $[Pd] = 1$. The numbers indicate experimental pressures. Solid lines obtained by elemental analysis. 0 Pd content in catalyst before experiments

this condition, the concentrations of both hydrogen and substrate are practically constant throughout the whole catalyst particle. In the case of our palladium catalyst, which is supported inside a swollen microporous polymer, the kinetic regime is never achieved. Therefore, the dissolution of palladium stops only at the end of the reaction, when the concentration of substrate is so low that the concentration of hydrogen exceeds that of 4-nitrotoluene in the whole particle. The evolution of concentration profiles at increasing conversion (*i.e.*, at increasing time), as calculated from the model

TABLE IV

Hydrogenation of different aromatic nitro compounds (denotation is given in Symbols)

Substrate	Catalyst	Solvent	P	T	$\xi_{0.1\text{MPa}}^a$	Reference
2,4-DNT	5% Pd/C	MeOH	0.468	308	0.163 ^b	16
2,4-DNT	5% Pd/C	EtOH	0.1	278	0.07 – 0.3 ^c	17
3-CNT	1% Pt/C	MeOH	0.656	313	10.8 ^d	25
4-NT	0.5% Pde/P1 ^e	MeOH	0.1	298	0.7 ^f	13
4-NT	0.5% Pde/P2 ^g	MeOH	0.25	303	1.95 ^h	this paper
4-NT	0.5% Pde/P2 ^g	MeOH	0.5	303	1.2 ^h	this paper
4-NT	0.5% Pde/P2 ^g	MeOH	0.75	303	0.9 ^h	this paper

^a Reaction rate recalculated with respect to 1 kg of metal and 0.1 MPa, *i.e.* the rate divided by the reaction pressure, mol kg⁻¹s⁻¹; 2,4-dinitrotoluene; ^c 3-chloronitrobenzene; ^d 4-nitrotoluene; ^e microporous poly(*N,N*-dimethylacrylamide-*co*-2-methacryloxyethanesulfonate-*co*-*N,N'*-methylenebisacrylamide); ^f microporous sulfonated poly(styrene-divinylbenzene); ^g molar hydrogen consumption; ^h rate of consumption of 2,4-DNT at 1 250–5 000 mol_{2,4-DNT}/kg_{cat}; ⁱ calculated from the data in Fig. 2, ref.²⁷; ^j calculated from the data in Table II, ref.¹³; ^k reaction rates calculated with kinetic parameters as in Table II and divided by the hydrogen experimental pressure.

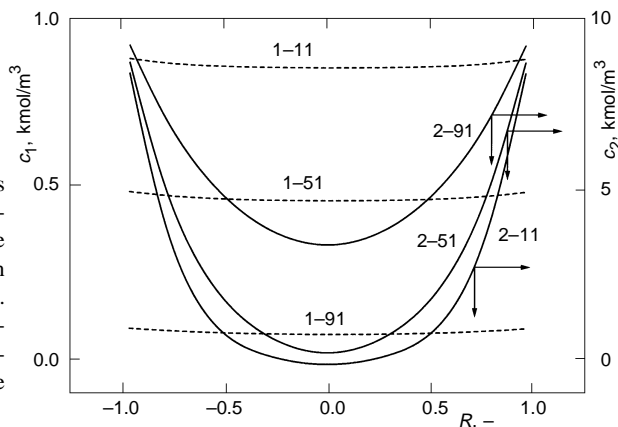


FIG. 4

Calculated concentration profiles of hydrogen (c_2) and 4-nitrotoluene (c_1) in the catalyst particle during the catalytic hydrogenation at 30 °C, 0.25 MPa and $[\text{Pd}] = 1$. The first number indicates the reactant (1 4-nitrotoluene, 2 hydrogen), the second, the conversion of 4-nitrotoluene in %

on the basis of the parameters given in Table III, is shown in Fig. 4; only at the end of the reaction, the particle is saturated with hydrogen and the dissolution of palladium is expected to stop.

Catalytic Activity of Various Pd Catalysts

The specific activity of several palladium catalysts, estimated from the values of reaction rates reported in the literature, are compared in Table IV. The first two entries refer to the hydrogenation of 2,4-dinitrotoluene. In accordance to the published reaction schemes^{16,17}, the hydrogenation of 2,4-dinitrotoluene starts with an attack on one nitro group, which enables to compare the starting reaction rate with that of the hydrogenation of 4-nitrotoluene. The rate of hydrogenation of 3-chloronitrobenzene²⁷ was introduced only as a curiosity, because a sulfur-poisoned partially deactivated Pt catalyst, was used in order to avoid the hydrogenolysis of the C-Cl bond. The next four entries refer to the hydrogenation of 4-nitrotoluene. It appears that the reduction of palladium(II) to metallic palladium with NaBH₄ in ethanol produces catalysts of lower activity¹³ than the reduction with hydrogen (this paper). It can also be seen that the catalyst investigated in this work exhibited the highest activity of all the catalysts referred to in Table IV.

CONCLUSIONS

The results presented in this and previous¹ papers and their comparison with the literature support the following conclusions:

1. In agreement with the literature²⁸, the extent of deactivation of Pd catalysts increases with decreasing concentration of hydrogen.
2. The assumption of the constant activity of Pd crystallites, independent of their size, was apparently wrong. In fact, the deactivation was much stronger than suggested on the basis of decreasing size of Pd crystallites; this means that during the deactivation, the most active sites (defects in crystal lattice, *e.g.* corners) are dissolved first, and the surface becomes smoother. This hypothesis is supported by the relatively high value of a_{Pd} in Eq. (4), the exponent with the palladium surface.
3. The dissolution of Pd and subsequent deactivation of the catalyst are due to its oxidation by 4-nitrotoluene. It can only occur in the presence of 4-aminotoluene, which is likely to form complexes with Pd(II). This enhances the oxidative power of the substrate and makes possible the palladium dissolution.
4. The stability of Pd-supported catalysts may be significantly increased by decreasing the diffusion resistance to transport of hydrogen to active sites, which can be accomplished by using low-metal catalysts, small catalyst particles, intensive mixing of the reaction mixture, optimum hydrogen pressure and optimum temperature (hydrogen solubility, reaction rate). These suggestions are valid both for organic and inorganic supported catalysts.

Knowledge of the investigated deactivation process could be improved by taking into account the size distribution of palladium crystallites. In this connection, Transmission Electron Microscopy (TEM) investigation of Pd catalysts could provide valuable precise data. Moreover, the TEM analysis of catalysts before and after catalytic tests could help to understand the changes in specific activity of palladium metal dispersed throughout the catalyst particle. From the theoretical point of view, study of formation of palladium amino complexes and the effect of steric hindrance caused by the polymer network should be of interest, too.

SYMBOLS

a_D	diffusion parameter in Eq. (8), kg/m^3
a_P	surface area of particles, m^2/m^3
a_j	exponents in the rate equations
c_i	concentration of component i , kmol/m^3
c_d	concentration of polymer chains in a certain domain of swollen polymer, nm/nm^3
D_i	diffusion coefficient of component i in a swollen polymer, m^2/s
$D_{i,0}$	diffusion coefficient of component i in the bulk solution, m^2/s
k_{LS}	liquid–solid mass-transfer coefficient, m/s
k_j	rate constant of reaction j
K_i	adsorption constant of component i , m^3/kmol
M_t	medium used for catalyst treatment
n_{rd}	number of repeated experiments with one catalyst
$n_{j,rd}$	number of points in the run j , rd
$n_{Pd,cr}$	number of Pd crystallites in a unit volume of the swollen catalyst, $1/\text{m}^3$
P_t	pressure of the catalyst treatment, MPa
[Pd]	palladium concentration in the reaction mixture, mol/m^3
r	radial coordinate, m
r_P	radius of swollen catalyst particles, m
$r_{Pd,cr}$	radius of Pd crystallites, m
R	dimensionless radial coordinate, $R = r/r_P$, m/m
S	swelling of the polymer, m^3/kg
s_{Pd}	surface of Pd crystallites in the swollen catalyst, m^2/m^3
t	time, s
t_t	time of the treatment of the catalyst, s
t_0	initial time for the solution of differential equations, s
T_t	temperature of the treatment of the catalyst, K
v_{H_2}	consumption of hydrogen, m^3
V_L	volume of bulk liquid, m^3
V_P	volume of swollen catalyst, m^3
V_d	specific volume of a polymer domain, cm^3/g
$w_{st,Pd}$	statistical weight on the Pd part of the minimization function
w_{Pd}	mass fraction of palladium in the dry resin, %
y	conversion of 4-nitrotoluene, %
ξ_V	rate of chemical reaction, $\text{kmol}/\text{m}^3\text{s}$
$\xi_{0.1\text{MPa}}$	reaction rate recalculated with respect to 1 kg of metal and 0.1 MPa, $\text{mol}/\text{kg s}$
ϵ_P	porosity of the catalyst

v_i	stoichiometric coefficient for component i
$\tau_{h, cen}$	half-time of the hydrogenation of cyclohexene, s
$\tau_{h, NT}$	half-time of the hydrogenation of 4-nitrotoluene, s
τ_{rc}	rotational correlation time of the probe, ps
SSE	sum of the squared residuals (squared errors in the minimum)

REFERENCES

1. Fiserá R., Kralik M., Annus J., Krátky V., Zecca M., Hronec M.: *Collect. Czech. Chem. Commun.* **1997**, 62, 1763.
2. Mackie J. S., Meares P.: *Proc. R. Soc. London, Ser. A* **1955**, 232, 498.
3. Biffis A., Corain B., Corvaja C., Jerabek K., Zecca M.: *J. Am. Chem. Soc.* **1995**, 117, 1603.
4. Biffis A., Corain B., Cvengrosová Z., Hronec M., Jerabek K., Kralik M.: *Appl. Catal.* **1996**, 142, 327.
5. Farin D., Avnir D.: *J. Am. Chem. Soc.* **1988**, 110, 2039.
6. Doraiswamy L. K., Sharma M. M.: *Heterogeneous Reactions: Analysis, Examples and Reactor Design*. Wiley, New York 1984.
7. Froment G. F., Hosten L. H. in: *Catalysis – Science and Technology* (J. R. Anderson and M. Boudart, Eds), Vol. 2, p. 97. Akademie-Verlag, Berlin 1983.
8. Albright R. L., Jakovac I. J.: *Catalysis by Functionalized Porous Organic Polymers*. ROHM and HAAS, Philadelphia 1985.
9. Wagner R., Lange P. M.: *Erdöl, Kohle, Erdgas* **1989**, 105, 414.
10. Jerabek K.: *ACS Symp. Ser.* **1996**, 635, 211.
11. Kralik M., Zecca M., Bianchin P., D'Archivio A. A., Galantini L., Corain B.: *J. Mol. Catal., Sect. A: Chem.* **1998**, 130, 95.
12. Biffis A., Corain B., Cvengrosová Z., Hronec M., Jerabek K., Kralik M.: *Appl. Catal.* **1995**, 124, 355.
13. Kralik M., Hronec M., Jorik V., Lora S., Palma G., Zecca M., Biffis A., Corain B.: *J. Mol. Catal.* **1995**, 101, 143.
14. Hronec M., Ilavský J.: *Chem. Papers* **1985**, 39, 705.
15. Haber F.: *Z. Elektrochem.* **1898**, 22, 506.
16. Janssen H. J., Kruithof A. J., Steghuis G. J., Westerterp K. R.: *Ind. Eng. Chem. Res.* **1990**, 29, 1822.
17. Neri G., Musolino M. G., Milone C., Signorino G.: *Ind. Eng. Chem. Res.* **1995**, 34, 2226.
18. Villadsen J., Michelsen M. J.: *Solution of Differential Equation Models by Polynomial Approximation*. Prentice Hall, Englewood Cliffs, NJ 1978.
19. Ashour S. S., Hanna O. T.: *Comput. Chem. Eng.* **1990**, 14, 267.
20. Flory P. J.: *Principles of Polymer Chemistry*. Cornell University Press, Ithaca, NY 1953.
21. Zecca M., Kralik M., Jerabek K., Galantini L., D'Archivio A. A., Corain B.: Unpublished results.
22. Jerabek K.: *Polymer* **1986**, 27, 971.
23. Cappillon J., Audebert R., Quivoron C.: *Polymer* **1985**, 26, 575.
24. Reid R. C., Prausnitz J. M., Poling B. E.: *The Properties of Gases and Liquids*. McGraw-Hill, New York 1987.
25. Hanika J., Sporka K., Ruzicka V., Deml J.: *Collect. Czech. Chem. Commun.* **1972**, 37, 951.
26. Radhakrishnan K., Ramachandran P. A., Brahme P. H., Chaudhari R. V.: *J. Chem. Eng. Data* **1983**, 28, 1.
27. Rode Ch. V., Chaudhari R. V.: *Ind. Eng. Chem. Res.* **1994**, 33, 1645.
28. Bird A. J., Thomson D. T. in: *Catalysis in Organic Synthesis* (W. H. Jones, Ed.), p. 61. Academic Press, New York 1980.